THE JOURNAL OF PHYSICAL CHEMISTRY A

Article

pubs.acs.org/JPCA

Compact MCTDH Wave Functions for High-Dimensional System-Bath Quantum Dynamics

M. Bonfanti,[†] G. F. Tantardini,[†] K. H. Hughes,[‡] R. Martinazzo,*[,†] and I. Burghardt*[,§]

[†]Dipartimento di Chimica, Università degli Studi di Milano, v. Golgi 19, 20133 Milano, Italy

[‡]School of Chemistry, Bangor University, Bangor, Gwynedd LL57 2UW, United Kingdom

[§]Institute of Physical and Theoretical Chemistry, Goethe University Frankfurt, Max-von-Laue-Strasse 7, 60438, Frankfurt, Germany

ABSTRACT: We employ a simple multiconfiguration time-dependent Hartree (MCTDH) ansatz tailored to an effective-mode transformation of environmental variables that brings the bath into a linear chain form. In this form, important (primary) degrees of freedom can be easily identified and treated at a high correlation level, whereas secondary modes are left uncorrelated. The resulting approach scales linearly with the bath dimensions and allows us to easily access recurrence times much longer than usually possible, at a very small computational cost. Test calculations for model atom−surface problems show that the system dynamics is correctly reproduced in the relevant time window, and quantitative agreement is attained for energy relaxation and sticking, particularly in non-Markovian environments. These results pave the way for tackling realistic system-bath quantum dynamical problems on the picosecond scale.

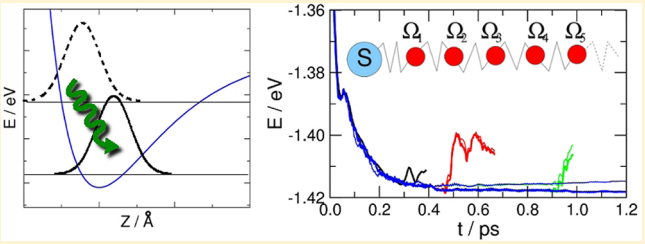

INTRODUCTION

The quest for efficient quantum dynamical methods able to handle high-dimensional systems is a long-standing issue in chemical dynamics, due to the well-known exponential scaling of conventional basis-set methods. Enormous progress has been made in this respect in the last two decades, particularly with the development of the multiconfiguration time-dependent Hartree (MCTDH) method,[1,2] which opened the door to comparatively large systems comprising 10−50 degrees of freedom, and describing a wide range of phenomena such as photodissociation[3−5] and photoabsorption spectra,[6,7] dissociation,[8,9] and reactive[10−13] and molecule−surface scattering.[14−17] Although the MCTDH method does not overcome the problem of the exponential growth of computational cost with system size, the method considerably alleviates the scaling problem by an optimal choice of basis functions which, in principle, can be systematically increased to give numerically exact solutions of the dynamical problem. Further improvements along these lines are obtained from multilayered variants of the MCTDH method which can handle several hundreds of degrees of freedom.[18−20]

Prompted by these developments, traditional open-system problems, where a "system" of interest can be clearly distinguished from its "environment", can now be tackled with "unitary" dynamical approaches, i.e., by following the unitary evolution of the system combined with a "bath" of harmonic oscillators chosen to represent the known statistical properties of the environment. Unitary approaches are attractive because they do not require specific approximations, contrary to quantum master equation approaches.[21,22] By the explicit treatment of the bath degrees of freedom, medium and strong system−bath coupling, non-Markovian effects, nonlinearities and anharmonicities in the bath and in the system-bath interaction, and initial correlations between the system and bath can be handled straightforwardly (i.e., limited only by the required numerical effort).

MCTDH has thus been applied to various system-bath dynamical problems,[23,24] but realistic systems still remain beyond current computational resources. In fact, hundreds of bath degrees of freedom are necessary to make the Poincaré recurrence time longer than any time of interest for the subsystem dynamics, and currently only the multilayer (ML) version of MCTDH[18−20] is feasible in such instances. Alternative routes are provided by a number of approximate schemes that have also been developed with the aim of improving the scaling with dimensionality. Among these is the Gaussian-based MCTDH (G-MCTDH) method,[25−27] which partially replaces the fully flexible single-particle functions with Gaussian functions, allowing considerable savings of both CPU time and random access memory by focusing attention on the most important degrees of freedom. Variants specifically designed for system-bath problems are the local coherent-state approximation (LCSA) method[28] and its generalization,[29] which extend the previous continuous-configuration time-dependent self-consistent field[30] method (see also ref 31) by introducing a simplified description of the bath dynamics while

Special Issue: Jörn Manz Festschrift

Received: June 29, 2012
Revised: August 25, 2012
Published: September 4, 2012

   dx.doi.org/10.1021/jp3064504 | J. Phys. Chem. A 2012, 116, 11406−11413

preserving as much as possible the important system-bath correlations.

Here we present a hierarchical approximate scheme that only involves standard MCTDH wave functions and can be easily applied to any system−bath problem. The key of the method is a recently introduced transformation of the bath degrees of freedom to a suitable chain form that sequentially unravels the response of the bath.[32−36] In this way, the environmental variables are naturally divided into two sets: those that are in close contact with the system and require a highly correlated treatment (primary modes) and those that play a secondary role and can be treated in a simplified way (secondary modes). We show here that, provided a sufficient number of modes are included in the primary set, the simple Hartree product chosen for the latter works rather well for typical problems, and does not require extra effort in coding or special attention in the dynamical simulations. This scheme is here applied for the first time in the context of effective-mode representations for typical system-bath models, with particular emphasis on the description of gas-surface dynamics. A similar development in the context of dynamics at conical intersections has been proposed in ref 37. Further developments in line with more approximate treatment of the secondary modes, e.g., using Gaussian basis sets,[26,28,38,39] will be considered in the near future.

The remainder of the paper is organized as follows. We first introduce the model problems, the corresponding Hamiltonians, the wave function ansatz, and some technical details. Following this, we report and discuss the numerical results and finally offer conclusions and an outlook.

THEORY

Model Hamiltonians. The basic model adopted in this work is the celebrated independent oscillator model, also known as the Caldeira−Leggett model,[22,40,41] where a system degree of freedom x (the "system") couples to a number N of harmonic oscillators q_k (the "bath"),

$$H = \frac{p^2}{2m} + V(x) + \sum_{k=1}^{N}\left\{\frac{{p_k}^2}{2} + \frac{1}{2}{\omega_k}^2\left(q_k - \frac{c_k f(x)}{{\omega_k}^2}\right)^2\right\} \tag{1}$$

Here the bath is represented in mass-weighted coordinates, p, $\{p_k\}$ are the corresponding momenta, m is the system mass, $V(x)$ is a bare system potential which is chosen to be of Morse form, $V(x) = D_e e^{-\alpha x}(e^{-\alpha x} - 2)$, and $f(x)$ is a coupling function[42]

$$f(x) = \frac{1 - e^{-\alpha x}}{\alpha}$$

such that $f(x) \approx x$ close to the equilibrium position, but with a finite limit as $x \to \infty$. The Morse potential parameters were set to $D_e = 1.55$ eV and $\alpha = 1.238\ {a_0}^{-1}$ and are representative of a hydrogen atom chemisorbed on a graphene layer;[39] correspondingly, in the following m is the mass of a H atom.

In this model, the frequencies of the bath oscillators ω_k and the coupling coefficients c_k can be chosen to sample a smooth spectral density $J_0(\omega) = m\omega \mathrm{Re}\tilde{\gamma}(\omega)$ characterizing a generalized Langevin equation[22,41,43] (GLE, here written for state-dependent friction)

$$m\ddot{x} = -V'(x) + f'(x)\times \left[\xi(t) - m\int_{-\infty}^{\infty}\gamma(t-\tau)\, f'(x(\tau))\, \dot{x}(\tau)\, d\tau\right]$$

where $\gamma(t)$ is the memory kernel, $\tilde{\gamma}(\omega)$ is its Fourier transform, $\tilde{\gamma}(\omega) \equiv \int_0^\infty \gamma(t)e^{i\omega t}\, dt$, and $\xi(t)$ is a Gaussian stochastic process with zero mean.

In this way, the Hamiltonian dynamics of eq 1 becomes equivalent[22,41] to the GLE for times inferior to the Poincaré recurrence time (T_{rec}) of the finite-size system. For a uniform sampling

$$\omega_k = k\Delta\omega \qquad c_k = \left(\frac{2\omega\Delta\omega J_0(\omega_k)}{\pi}\right)^{1/2}$$

T_{rec} takes the simple form $T_{rec} = 2\pi/\Delta\omega = 2\pi N/\omega_c$, thereby increasing linearly with the number of bath modes if a maximum (cutoff) frequency ω_c is fixed on physical grounds. This implies that an exponential growth of computational effort is to be expected if eq 1 is used in quantum dynamical simulations aiming at longer and longer times.

Equivalently,[35] the continuum limit of eq 1 can be represented in a linear chain form involving the effective modes $\{X_n\}_{n=1}^{\infty}$, namely

$$H = \frac{p^2}{2m} + V(x) + \Delta V(x) - D_0 f(x) X_1 + \frac{1}{2}\sum_{n=1}^{\infty}\{{P_n}^2 + {\Omega_n}^2{X_n}^2\} - \sum_{n=1}^{\infty} D_n X_n X_{n+1} \tag{2}$$

where $\{P_n\}_{n=1}^{\infty}$ are the conjugate momenta, $\Delta V(x)$ is a renormalization potential

$$\Delta V(x) = \frac{m\delta\Omega^2}{2}x^2 \qquad m\delta\Omega^2 = \frac{2}{\pi}\int_0^\infty \frac{J_0(\omega)}{\omega}\, d\omega$$

and $\{D_n,\Omega_{n+1}\}_{n=0}^{\infty}$ are effective mode coupling coefficients and frequencies, respectively. The latter read as

$${D_n}^2 = \frac{2}{\pi}\int_0^\infty \omega J_n(\omega)\, d\omega$$

$${\Omega_{n+1}}^2 = \frac{2}{\pi {D_n}^2}\int_0^\infty \omega^3 J_n(\omega)\, d\omega$$

where $J_n(\omega)$ (the spectral density felt by the nth mode as a consequence of its interaction with the remainder of the chain) follows from a simple one-term recurrence,[35] which can be started with $J_0(\omega)$.

The chain modes thus introduced effectively perform a Markovian embedding of the dynamics[35] and sequentially unravel the memory kernel in time,[36] thereby providing a powerful tool to describe (non-Markovian) ultrafast phenomena by means of either reduced-dimensional models or Markovian master equations for an enlarged system.[32,44−46] This approach has important predecessors in the seminal work by Mori[47,48] as well as related developments by Adelman[49] and others.

As we show below, the effective modes further offer the opportunity of tackling long time problems in explicit dynamical studies of the composite system.

Wave Function Ansatz. For the model Hamiltonians of eqs 1 and 2 high-dimensional wavepacket dynamics as implemented in the MCTDH method (Heidelberg package)[50]

dx.doi.org/10.1021/jp3064504 | J. Phys. Chem. A 2012, 116, 11406−11413

are performed to investigate typical (zero-temperature) dissipative problems to be discussed below. In the MCTDH method, the wave function is written as a combination of variationally optimal time-dependent Hartree products which, for the bath in normal form (i.e., according to eq 1), we take as

$$\Psi(x,q_1,...,q_N) = \sum_{i_0 i_1 .. i_P} c_{i_0 i_1 ... i_P} \psi_{i_0}(x)\, \Phi_{i_1}^{(1)}(Q_1)...\Phi_{i_P}^{(P)}(Q_P)$$

where Q_1, Q_2, ..., Q_P are "combined" modes that can comprise more than one bath coordinate q_k, e.g., $Q_1 = \{q_1 q_2 ... q_m\}$, $\{\psi_i\}_{i=1}^{n_0}$'s are single-particle functions (spf's) for the test system, and $\{\Phi_i^{(k)}\}_{i=1}^{n_k}$ are spf's for the kth mode. In the calculations to be discussed below we used $N = 50$ bath modes and typically combined them in groups of five, setting $n_0 = 5-14$ for the system and $n_k = 3-14$ for the bath modes. These numbers are a good compromise between accuracy and computational cost and resulted from extensive convergence tests performed at a preliminary stage.

This approach has a limit of ~100 modes that can be handled with present computational resources, unless multilayer MCTDH approaches are considered. To overcome these difficulties with the standard MCTDH method, we take advantage of the linear chain form of the bath (eq 2), and identify a number N_P of primary modes that closely couple to the system, $\{X_n\}_{n=1}^{N_P}$. These modes are treated exactly by a full, many particle expansion, whereas the remaining (secondary) modes are described by a single spf per mode (Hartree approximation), i.e.

$$\Psi(x,X_1,X_2,...,X_N) = \Phi_P \phi^{(N_P+1)}(X_{N_P+1})...\phi^{(N)}(X_N)$$

where $\Phi_P \equiv \Phi(x,X_1,X_2,...,X_{N_P})$ is a full MCDTH wave function like the one given above, but now restricted to the system modes plus primary effective degrees of freedom (DOFs). We call this a "partially correlated" chain description. In this way, the computational effort scales exponentially only with the number of *primary* modes, and is $O(N)$ as a function of the number of secondary modes. We typically grouped the primary modes in 2−3-dimensional particles, and as we show below, setting $N_P = 10-15$ we obtain satisfactory results for the problems considered. N could thus be increased up to several hundred to easily attain recurrence times of several pico-seconds, which is of the order needed to address typical problems in condensed phase systems.

Spectral Densities. We considered two typical spectral densities representative of non-Markovian dynamics. The first is the Lorentzian introduced by Garg et al.[51] (SD1),

$$J(\omega) = \frac{{d_0}^2}{m_0} \frac{\gamma\omega}{({\omega_0}^2 - \omega^2)^2 + \gamma^2\omega^2}$$

which describes the non-Markovian environment felt by a particle interacting with a harmonic oscillator of frequency ω_0 and mass m_0, which in turn couples to an Ohmic bath with relaxation time γ^{-1}. The second spectral density (SD2), illustrated in Figure 1, is a more structured and realistic spectral density obtained from energy-gap fluctuations in an oligo-phenylene-vinylene system, computed with molecular dynamics simulations;[52] here, some structure was added in the high-frequency region (i.e., a "bump" around 2500 cm^{-1}) to obtain a more complex frequency dependence.

In addition, we considered several truncated Ohmic models, $J(\omega) = m\omega\gamma$ for $\omega \le \omega_c$ and zero otherwise, for $\gamma^{-1} = 50-200$, fs as characteristic of (quasi-)Markovian behavior. The cutoff frequency was set to $\omega_c = 0.02$ au, and the same cutoff was used for the Lorenztian model above; for the latter, we also set $\omega_0 = 0.1$ au, $\gamma^{-1} = 50$ fs and ${d_0}^2/m = 1.497 \times 10^{-6}$ au, in a such a way that D_0 had the same value as in a truncated Ohmic model with $\gamma^{-1} = 50$ fs. For SD2 we set a similar cutoff frequency, $\omega_c = 5000$ cm^{-1}, i.e., $\omega_c = 0.02278$ au.

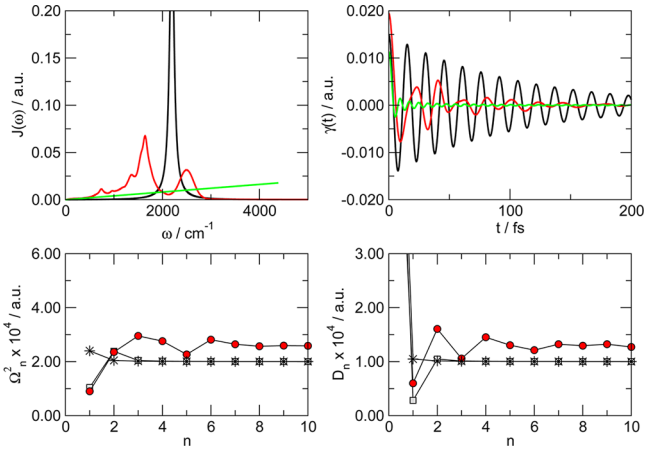

Figure 1. Spectral densities used in this work. Top: (left) spectral densities for the non-Markovian models discussed in the main text (black and red for SD1 and SD2, respectively), along with that of a truncated Ohmic model for $\gamma^{-1} = 50$ fs (green); (right) corresponding memory kernels relating to the GLE. Bottom: effective mode (squared) frequencies (left) and couplings (right) for the models above (squares, circles, and stars, respectively).

Note that we refer to the Ohmic case as quasi-Markovian because an Ohmic spectral density still implies colored noise in a quantum-mechanical setting.[22] Also, the frequency cutoff ω_c introduces non-Markovian behavior at times shorter than ω_c^{-1}.

Figure 1 shows the non-Markovian spectral density models, along with the corresponding memory kernels and effective mode parameters.

Dynamical Problems. To illustrate the dynamics in the transformed representation, we have studied two problems that are prototypical of atom−surface interactions. The first is the small amplitude, damped motion of an anharmonic (Morse) oscillator initially displaced from its equilibrium position. In this case, we typically followed the evolution of the system energy (corrected for half of the coupling with the bath[23,24]), and further considered the position correlation function,

$$C_x(t) = \langle x(t)\, x(0)\rangle = \langle \Psi_0 | e^{iHt} x e^{-iHt} x | \Psi_0 \rangle$$

(where $x(t)$ is a Heisenberg-picture operator) that requires two wavepacket propagations at a time, namely $|\Psi_t\rangle = e^{-iHt}|\Psi_0\rangle$ and $|\Phi_t\rangle = e^{-iHt}x|\Psi_0\rangle$.

In the second type of dynamical problem, we initially placed the Morse oscillator at a large distance from its equilibrium position (here, at 6.35 Å), in the asymptotic region of the potential, to mimic a particle impinging on a surface with some given momentum. In this case we followed the fraction of the wavepacket which gets trapped in the interaction region as a consequence of the interaction with the bath,

$$P_B(t) = \sum_\nu \mathrm{Tr}(P_\nu |\Psi(t)\rangle\langle\Psi(t)|) \qquad (3)$$

where Tr is the trace operation and $P_\nu = |\nu\rangle\langle\nu|$ projects onto the νth bound state in the Morse potential well. In this case a

dx.doi.org/10.1021/jp3064504 | J. Phys. Chem. A 2012, 116, 11406−11413

complex absorbing potential was added at large x to prevent the reflected part of the wave function from producing artifacts in the trapping probability. We chose a quadratic absorbing potential with length ~5.5 au and a strength in the range $\eta = (8-120) \times 10^{-5}$ au, for an initial momentum of the H atom in the range 4−12 au.

In each case considered, we took a product state initial wave function,

$$\Psi_0(x, \{q_k\}) = \psi_0(x)\, \Phi(\{q_k\})$$

where the bath wave function $\Phi(\{q_k\})$ was chosen to be the ground state of a hypothetical bath interacting with a classical system positioned at $x_0 = \langle\psi_0|x|\psi_0\rangle$. The latter is of product form for the normal form eq 1 of the bath. For the bath in the linear chain representation, we performed imaginary time-propagation to find the corresponding ground state.

RESULTS AND DISCUSSION

Small Amplitude Vibrations. We first consider the small amplitude, damped motion of the Morse oscillator. Figure 2 shows the evolution of the system energy when the Morse oscillator (MO) is initially displaced from its equilibrium position, with two different non-Markovian environments (left and right panels for SD1 and SD2, respectively). Results for the bath in linear chain form, all with $N = 100$ and different numbers of primary modes $N_P = 5, 10, 15$ as detailed in the caption of Figure 2, are compared with those obtained with the usual prescription, eq 1, for $N = 50$. The latter are well-converged with respect to the number of spfs and can be considered numerically exact for the dissipative problems at hand for times less than the recurrence time (here $T_{rec} \approx 300$ *fs*).

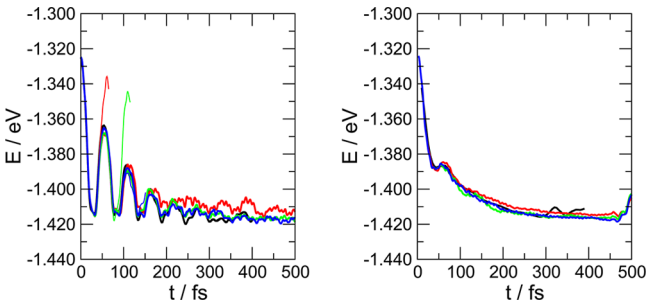

Figure 2. Small amplitude motion. Evolution of the system energy for the two non-Markovian models described in the text (left and right panel for SD1 and SD2, respectively), using the first $N = 100$ effective modes. Results for $N_P = 5, 10, 15$ (red, green, blue, respectively) are compared with the benchmark (bath in normal form), given by the black line. In the left panel, thin lines represent results for truncated chains $N = N_P = 5, 10, 15$, with the same color code.

Also shown for comparison (left panel) are the results obtained for fully correlated truncated models, i.e., when $N = N_P = 5, 10, 15$, for times slightly longer than the recurrence times of the truncated chains. These results demonstrate numerically that, when the effective modes are treated exactly in the dynamics, the response of the bath is very accurately reproduced over time scales that depend on the length of the chain, a result previously obtained by analyzing the corresponding GLE.[36]

For longer times, the effect of the finiteness of the chain becomes evident in the artificial flow of energy back to the system. Figure 2 shows that this reflected flow may be corrected by adding further (secondary) modes and treating them at a single particle (Hartree) level, provided a sufficient number of primary modes are considered. Results for $N_P = 5, 10, 15$ primary modes out of $N = 100$ total modes are exceptionally good for times much longer than those of the corresponding truncated chains. The net effect is that T_{rec} can be pushed to significantly longer times, at much lower cost due to the linear scaling properties in the secondary subspace.

This shows that, at least in the examples considered here, a large number of modes play only a "dissipative role" and can be treated at a simplified level without corrupting the system behavior. The effective mode transformation plays a central role in identifying these modes that are otherwise mixed with the important, primary modes in the standard normal mode representation of the bath Hamiltonian, eq 1.

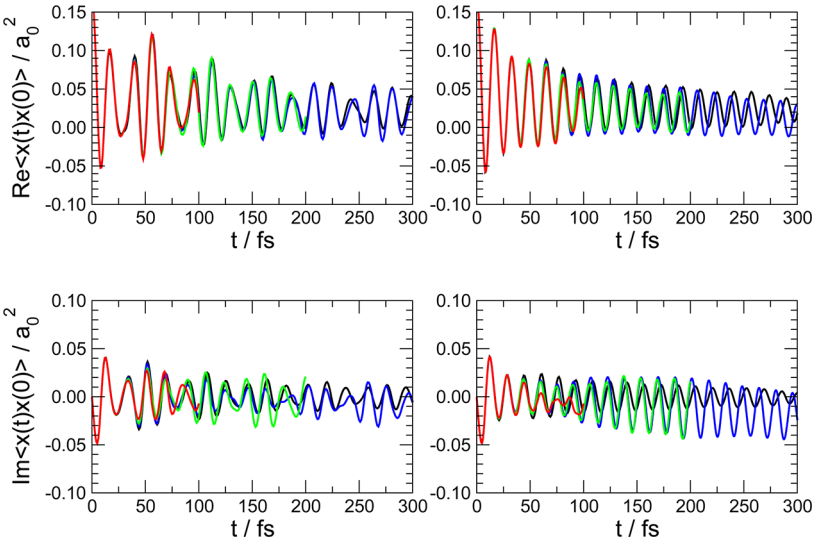

Figure 3. Real (top) and imaginary (bottom) parts of the position autocorrelation function for the two non-Markovian models considered in the main text (left and right for SD1 and SD2, respectively). Red, green, and blue lines for $N_P = 5, 10, 15$ and black lines for the benchmark calculations.

dx.doi.org/10.1021/jp3064504 | J. Phys. Chem. A 2012, 116, 11406−11413

Such a good agreement is not limited to averaged quantities like the system energy or the mean position and width of the wavepacket along the MO coordinate (data not shown). Figure 3 shows for instance the evolution of the position autocorrelation for the two non-Markovian models considered above, with different numbers of primary degrees of freedom. Results are shown only up t = 100, 200, 300 fs for N_P = 5, 10, 15, respectively, for the sake of clarity, but they are reasonably good (when compared to the benchmark) over the whole time window considered. This is particularly true for the imaginary part of the autocorrelation function, which is a genuine quantum object. Deviations from the exact results at long times become noticeable, even though they are tolerable, especially in light of the computational cost of the calculations (see below).

For comparison we also considered two (quasi) Markovian cases, the truncated Ohmic spectral densities with relaxation times γ^{-1} = 50 and 100 fs. Results are given in Figures 4 and 5

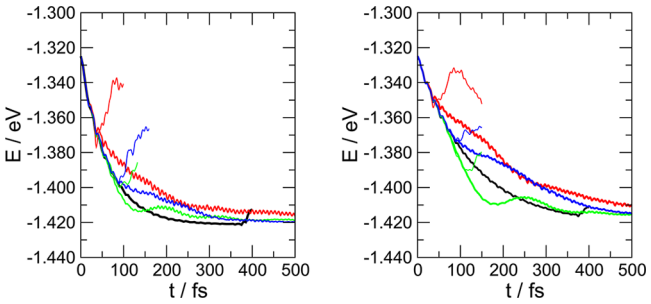

Figure 4. Same as in Figure 2 for two Ohmic models, γ^{-1} = 50, 100 fs (left and right panel, respectively). Red, green, and blue lines for N_P = 5, 10, 15 and black lines for the benchmark calculations. As in Figure 2, thin lines represent results for truncated chains $N = N_P$ = 5, 10, 15 for comparison.

for the truncated chains $N = N_P$ = 5, 10, 15, and for the partially correlated chains with the same number of primary modes and N = 100, along with benchmarks. Here the agreement is not as good as observed above for the non-Markovian models, and an artificial non-Markovian behavior becomes evident for the partially correlated chain. This behavior is due to the uneven correlation treatment of chains that are uniform for an Ohmic model, as shown for instance by the effective mode parameters reported in Figure 1. The approximate treatment necessarily introduces an effective non-Markovian behavior that shows up as a deviation from the smooth exponential decay of the energy and of the envelope of the position autocorrelation. Thus, in this case, unless the required number of primary modes is sufficient to cover a time window 2−3 times larger than γ^{-1}, some deviation from the Markovian exponential decay is expected.

We have not yet understood how to minimize this correlation-related non-Markovian behavior of the approximate chains, without increasing the number of primary modes. It seems, though, that (differently from the non-Markovian models discussed above) there is a *continuous* flow of energy to the "secondary" modes, which thus saturate before dissipating energy to their neighbors. If this is the case, ad hoc correlation schemes that smoothly interpolate between primary and secondary modes prescriptions may help in removing dynamical bottlenecks in the energy flow. However, we did not investigate this point further because Markovian models hardly apply to realistic situations, especially in the context of ultrafast molecular processes. Further, quasi-exact master equations can be employed in this limit that are solvable with standard techniques.

Sticking. Next we consider the paradigm "sticking" problem where the system initially placed in the asymptotic region is launched toward the region of small x where it starts to interact with the bath (the "surface"). As a result of the interaction, a fraction of the "system wavepacket" becomes trapped in the interaction region and eventually undergoes a relaxation dynamics similar to that described above, whereas the remaining fraction goes back into the asymptotic region. Despite its simplicity, this kind of process necessitates a correlated description of the dynamics: the above wavepacket splitting cannot be captured by any mean-field approximation, which thus badly fails in describing the dynamics even qualitatively. Notice further that for the model to be sound the choice of the coupling function with a correct limiting behavior is essential.

The results for the sticking probability P_S in the two non-Markovian models described above, as well as those for two quasi-Markovian environments (γ^{-1} = 100, 200 fs) are shown in Figure 6, in the energy range 0.5−1 eV. P_S has been extracted as the long time limit of the population of the system bound states, $P_S = \lim_{t\to\infty} P_B(t)$ where P_B is defined in eq 3, and each energy point corresponds to a wavepacket with an incident energy distribution peaked around its mean value. Similar results are expected for an appropriate energy-resolved analysis of a wavapacket dynamics covering the whole energy range.

Parallel to the previous analysis, we compare in Figure 6 the results of the approximate calculations with N_P = 5, 10, 15 and N = 100 with those of the benchmark. No truncated model makes sense here, because sticking require a fully dissipative bath.

As is evident from Figure 6, the results steadily converge toward the correct values when the number of primary modes increases, irrespective of the environment model. In particular,

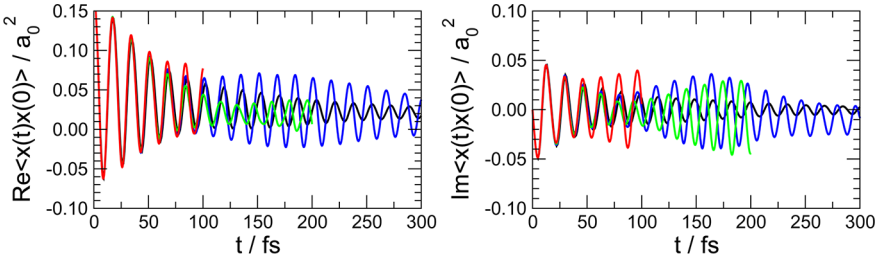

Figure 5. Same as in Figure 3 for an Ohmic bath model with γ^{-1} = 50 fs. Red, green, and blue lines for N_P = 5, 10, 15 and black lines for the benchmark calculations.

dx.doi.org/10.1021/jp3064504 | J. Phys. Chem. A 2012, 116, 11406−11413

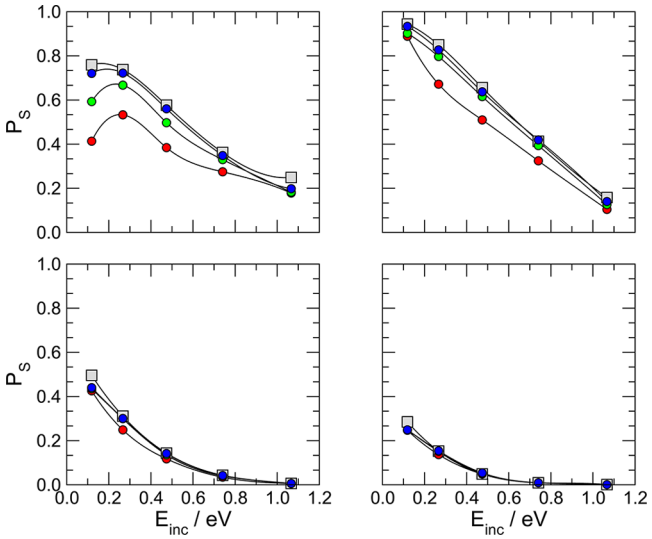

Figure 6. Sticking probability as a function of the incident energy, for the two non-Markovian models of the main text (top row, left and right panel for SD1 and SD2, respectively) and for two Ohmic bath models with γ^{-1} = 100, 200 fs (bottom row, left and right panel, respectively). Squares are benchmark results obtained with the bath in normal form and red, green and blue circles are for N_P = 5, 10, 15, respectively. Lines are spline interpolations of the data.

for N_P = 5 the correct shape of the sticking curve is recovered (at a very low computational cost, see below) and, for N_P in the range 10−15 the computed sticking probability agrees quantitatively with the exact one to within ∼1% for all but the lowest incident energy.

This contrasts with our previous results on vibrational relaxation dynamics, which showed that Ohmic models tend to perform worse than non-Markovian ones. Indeed, in this direct scattering process a correct sticking probability requires only that dissipation of energy during the first round trip of the projectile into the interaction region is well described. This is an impulsive process that hardly saturates the bath modes, if treated approximately in a linear chain representation. The detailed way in which the trapped component relaxes toward the ground state in the well is irrelevant for the total sticking probability. The main issues here are thus the short-time relaxation dynamics during the collision and a long recurrence time necessary to reach a well-defined long-time limit, both well captured by our partially correlated chain description.

In contrast, in approximate treatments with the bath in normal form, saturation of the low-frequency modes is likely to occur, and sticking probabilities are generally smaller than the exact ones.[29]

COMPUTATIONAL PERFORMANCE

To better appreciate the results of the previous sections, it is worth mentioning that the calculations with the partially correlated chains are considerably less time-consuming than the normal bath benchmarks. Table 1 reports the timings for the SD2 model of the environment, for the vibrational relaxation dynamics discussed above. The values refer to a standard workstation with Intel Xeon CPUs E5430@2.66 GHz and should be compared with a 400 fs propagation of the corresponding normal bath, which required 11 562 CPU seconds for N = 50 modes. Similar results hold for the memory requirements.

Table 1. CPU Times of the Vibrational Relaxation Dynamics in the SD2 Model for the Environment, for a 1 ps Simulation Time

N	N_P = 10	N_P = 15
100	616 s	1746 s
200	818 s	3034 s
300	1079 s	3985 s

Apart from the absolute amount of time, which is clearly much smaller for linear chains, the most promising feature of the partially correlated approach presented here is the scaling with the length of the part of chain, which is treated at a single spf (Hartree) level, which is approximately linear. This means, in turn, that the recurrence time of the finite-size model is only a linear function of the CPU time. This is shown in Figure 7,

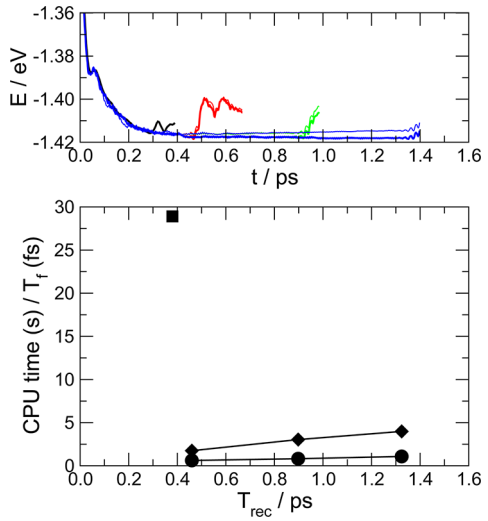

Figure 7. Top: energy relaxation in the non-Markovian model SD2, for different total number of effective modes, N = 100, 200, 300 (red, green and blue, respectively) and N_P = 10, 15 (thin and thick lines), along with the benchmark in normal form for N = 50. The "blowing up" of the energy curves signals the recurrence times of the finite-size model. Bottom: CPU timings (in real seconds per femtosecond of simulation) vs the recurrence time estimated from the top graph, for N_P = 10 (circles) and N_P = 15 (diamonds). The square is the corresponding value for the benchmark.

where the CPU time needed for a given simulation time is reported as a function of the estimated recurrence time of the bath. The latter was extracted by looking at energy decay curves shown in the top panel as the time where energy goes back to the system and is approximately given by the longest (quasi) period of the truncated chain. Also reported, for comparison, are the corresponding values for the bath in normal form, where an increase of T_{rec} is accompanied by an exponential increase of computational cost.

CONCLUSIONS

In this work, we considered the vibrational relaxation and sticking processes for an anharmonic (Morse) oscillator coupled to a thermal bath describing the environment, in accordance with the well-known independent oscillator model of dissipative dynamics. Using the MCTDH method, we studied these dynamical phenomena comparing the normal-form representation (eq 1) of the bath degrees of freedom with

dx.doi.org/10.1021/jp3064504 | J. Phys. Chem. A 2012, 116, 11406−11413

a novel, effective-mode based, linear chain representation (eq 2) of the bath.[32,35,36,45,46]

This equivalent chain formulation of the independent oscillator Hamiltonian allows us to introduce an approximation scheme in which a large number of oscillators can be included. In this "partially correlated chain" scheme, the number of modes that are fully correlated is rather small, and the majority of modes are treated at a Hartree level. Within the standard MCTDH framework, this approximate description is conveniently applied by using a single spf for the mean-field part of the chain.

For the relaxation problems considered, we followed the evolution of typical averages such as the system energy and the position correlation, starting from an initial condition where the oscillator was displaced from its equilibrium position. We found that the exact short-time dynamics could be reproduced with reduced-dimensional models where the chain is truncated at some point. For longer times, we found that the simplified, mean-field description of the remaining chain modes gives very satisfactory results, particularly for non-Markovian relaxation models.

The corresponding computational cost is modest and increases *linearly* with the dimension of the secondary bath. This is in contrast to fully correlated calculations that are subject to an exponential scaling (and which are often found to require a larger cost for chain models as compared with pretransformed normal-mode models). Hence, very long recurrence times become possible with the proposed "partially correlated" scheme using standard MCTDH techniques.

We further considered a model sticking problem, where the above properties (exact short time dynamics and long recurrence times) are already sufficient to correctly describe impulsive sticking. Results with several bath models showed excellent agreement at a very low computational cost, irrespective of the type of environment, and suggest that the full quantum description of realistic gas−surface problems can be quantitatively addressed in the near future with the proposed approach. Possible extensions of the effective mode approach to anharmonic system-bath couplings, which would be of key importance, e.g., for vibrational energy relaxation of high-frequency modes mediated by cubic anharmonicities, could be addressed along the lines of ref 53.

Prospectively, the method can be of help in many complex situations occurring in condensed phase systems. For instance, in exciton dynamics, excitation is transferred among a number of sites, each having their own environment. A simplified description where N_p = 5−10 (out of $N \approx 100$) per site is feasible with the present computational resources for some tens of sites and would allow one to quantitatively describe energy transfer and decoherence in realistic models without incurring finite-size effects.

AUTHOR INFORMATION

Corresponding Author

*E-mail: R.M., rocco.martinazzo@unimi.it; I.B., burghardt@theochem.uni-frankfurt.de.

Notes

The authors declare no competing financial interest.

REFERENCES

(1) Beck, M. H.; Jackle, A.; Worth, G. A.; Meyer, H.-D. *Phys. Rep.* **2000**, *324*, 1.
(2) Meyer, H.-D.; Gatti, F.; Worth, G. A., Eds. *Multidimensional Quantum Dynamics: MCTDH Theory and Applications*; Wley-VCH Verlag: Weinheim, 2009.
(3) Hammerich, A. D.; Manthe, U.; Kosloff, R.; Meyer, H.-D.; Cederbaum, L. S. *J. Chem. Phys.* **1994**, *101*, 5623.
(4) Liu, L.; Fang, J. Y.; Guo, H. *J. Chem. Phys.* **1995**, *102*, 2404.
(5) Pouilly, B.; Monnerville, M.; Gatti, F.; Meyer, H.-D. *J. Chem. Phys.* **2005**, *122*, 184313.
(6) Köppel, H.; Döscher, M.; Baldea, I.; Meyer, H.-D.; Szalay, P. G. *J. Chem. Phys.* **2002**, *117*, 2657.
(7) Gromov, E. V.; Trofimov, A. B.; Vitkovskaya, N. M.; Köppel, H.; Schirmer, J.; Meyer, H.-D.; Cederbaum, L. S. *J. Chem. Phys.* **2004**, *121*, 4585.
(8) Fang, J. Y.; Guo, H. *J. Chem. Phys.* **1994**, *101*, 5831.
(9) Meier, C.; Manthe, U. *J. Chem. Phys.* **2001**, *115*, 5477.
(10) Matzkies, F.; Manthe, U. *J. Chem. Phys.* **1997**, *106*, 2646.
(11) Jäckle, A.; Heitz, M. C.; Meyer, H.-D. *J. Chem. Phys.* **1999**, *110*, 241.
(12) Huarte-Larrañaga, F.; Manthe, U. *J. Chem. Phys.* **2000**, *113*, 5115.
(13) Sukiasyan, S.; Meyer, H.-D. *J. Chem. Phys.* **2002**, *116*, 10641.
(14) Ehara, M.; Meyer, H.-D.; Cederbaum, L. S. *J. Chem. Phys.* **1996**, *105*, 8865.
(15) Milot, R.; Jansen, A. P. J. *J. Chem. Phys.* **1998**, *109*, 1966.
(16) Heitz, M.; Meyer, H.-D. *J. Chem. Phys.* **2001**, *114*, 1382.
(17) van Harrevelt, R.; Manthe, U. *J. Chem. Phys.* **2004**, *121*, 3829.
(18) Wang, H.; Thoss, M. *J. Chem. Phys.* **2003**, *119*, 1289.
(19) Wang, H.; Thoss, M. In *Multidimensional Quantum Dynamics: MCTDH Theory and Applications*; Meyer, H.-D., Gatti, F., Worth, G. A., Eds; Wiley-VCH: 2009; Chapter 14.
(20) Manthe, U. *J. Chem. Phys.* **2008**, *128*, 164116.
(21) Breuer, H. P.; Petruccione, F. *The theory of open quantum systems*; Oxford University Press, New York, 2002.
(22) Weiss, U. *Quantum Dissipative Systems*, 3rd ed.; World Scientific: Singapore, 2008.
(23) Nest, M.; Meyer, H.-D. *J. Chem. Phys.* **2003**, *119*, 24.
(24) Burghardt, I.; Nest, M.; Worth, G. A. *J. Chem. Phys.* **2003**, *119*, 5364.
(25) Burghardt, I.; Meyer, H.-D.; Cederbaum, L. S. *J. Chem. Phys.* **1999**, *111*, 2927.
(26) Worth, G. A.; Burghardt, I. *Chem. Phys. Lett.* **2003**, *368*, 502.
(27) Worth, G. A.; Robb, M. A.; Burghardt, I. *Faraday Discuss* **2004**, *127*, 307.
(28) Martinazzo, R.; Nest, M.; Saalfrank, P.; Tantardini, G. F. *J. Chem. Phys.* **2006**, *125*, 194102.
(29) López-López, S.; Nest, M.; Martinazzo, R. *J. Chem. Phys.* **2011**, *134*, 014102.
(30) Zhang, D. H.; Bao, W.; Yang, M. *J. Chem. Phys.* **2005**, *122*, 091101.
(31) López-López, S.; Nest, M. *J. Chem. Phys.* **2010**, *132*, 104103.
(32) Cederbaum, L. S.; Gindensperger, E.; Burghardt, I. *Phys. Rev. Lett.* **2005**, *94*, 113003.
(33) Hughes, K. H.; Christ, C. D.; Burghardt, I. *J. Chem. Phys.* **2009**, *131*, 024109.
(34) Hughes, K. H.; Christ, C. D.; Burghardt, I. *J. Chem. Phys.* **2009**, *131*, 124108.
(35) Martinazzo, R.; Vacchini, B.; Hughes, K. H.; Burghardt, I. *J. Chem. Phys.* **2011**, *134*, 011101.
(36) Martinazzo, R.; Hughes, K. H.; Burghardt, I. *Phys. Rev. E* **2011**, *84*, 030102.
(37) Basler, M.; Gindensperger, E.; Meyer, H.-D.; Cederbaum, L. S. *Chem. Phys.* **2007**, *347*, 78.
(38) Burghardt, I.; Nest, M.; Worth, G. A. *J. Chem. Phys.* **2003**, *119*, 5364.
(39) Chapman, C. T.; Cheng, X.; Cina, J. A. *J. Chem. Phys. A* **2011**, *115*, 3980.
(40) Caldeira, A. O.; Leggett, A. J. *Phys. Rev. A* **1985**, *31*, 1059, DOI http://link.aps. org/doi/10.1103/PhysRevA.31.1059.

(41) Pottier, N. *Nonequilibrium statistical physics: linear irreversible processes, Oxford Graduate Texts*; Oxford University Press: Oxford, U.K., 2010; URL http://books. google.com/books?id=mf584x_P94AC.
(42) Nest, M.; Meyer, H.-D. *J. Chem. Phys.* **2003**, *119*, 24.
(43) Ford, G. W.; Lewis, J. T.; O'Connell, R. F. *Phys. Rev. A* **1988**, *37*, 4419.
(44) Tamura, H.; Bittner, E. R.; Burghardt, I. *J. Chem. Phys.* **2007**, *126*, 021103.
(45) Hughes, K. H.; Christ, C. D.; Burghardt, I. *J. Chem. Phys.* **2009**, *131*, 024109.
(46) Hughes, K. H.; Christ, C. D.; Burghardt, I. *J. Chem. Phys.* **2009**, *131*, 124108.
(47) Mori, H. *Prog. Theor. Phys.* **1965**, *33*, 423.
(48) Mori, H. *Prog. Theor. Phys.* **1965**, *34*, 399.
(49) Adelman, S. A. *Adv. Chem. Phys.* **1980**, *44*, 143.
(50) Worth, G. A.; Beck, M. H.; A. Jäckle, Meyer, H.-D. *The MCTDH Package*, Version 8.4, 2007. See http://mctdh.uni-hd.de.
(51) Garg, A.; Onuchic, J. N.; Ambegaokar, V. *J. Chem. Phys.* **1985**, *83*, 4491.
(52) Sterpone, F.; Martinazzo, R.; Panda, A. N.; Burghardt, I. *Z. Phys. Chem.* **2011**, *225*, 541.
(53) Vibók, Á.; Csehi, A.; Gindensperger, E.; Köppel, H.; Halász, G. J. *J. Phys. Chem. A* **2012**, *116*, 2629.